

## Two exonic elements in the flanking constitutive exons control the alternative splicing of the $\alpha$ exon of the ZO-1 pre-mRNA

Rebeca Martínez-Contreras<sup>a</sup>, José Manuel Galindo<sup>b</sup>, Arturo Aguilar-Rojas<sup>c</sup>, Jesús Valdés<sup>b,\*</sup>

<sup>a</sup>Departamento de Fisiología, Biofísica y Neurociencias, CINVESTAV-México, Apartado Postal 14-740, México DF 07000, México

<sup>b</sup>Departamento de Bioquímica, CINVESTAV-México, Apartado Postal 14-740, México DF 07000, México

<sup>c</sup>Departamento de Biomedicina Molecular, CINVESTAV-México, Apartado Postal 14-740, México DF 07000, México

Received 18 September 2002; received in revised form 16 September 2003; accepted 19 September 2003

### Abstract

The 240-bp  $\alpha$  exon of the tight junction (TJ) protein ZO-1 pre-mRNA is alternatively spliced. Expression of both ZO-1 $\alpha$ + / ZO-1 $\alpha$  – isoforms results in hermetic TJs, and these become leaky when ZO-1 $\alpha$  – expression prevails. The  $\alpha$  exon inclusion/skipping mechanism was studied by *in vivo* RT-PCR splicing assays in neural and epithelial cells, utilizing a canine minigene construct containing the  $\alpha$  exon, and the flanking introns and exons. Inclusion of the  $\alpha$  exon always occurs in wild-type MDCK cells and it is detectable in transfected HeLa cells. However, the  $\alpha$  exon is skipped in transfected neural cells. Accordingly, both 5' and 3' splice sites surrounding the  $\alpha$  exon appear to be suboptimal and no *cis*-acting splicing control elements were found in this exon. Deletion analysis revealed an 83-bp splicing enhancer in the downstream exon and a 35-bp splicing silencer at the beginning of the upstream exon. In epithelial cells all constructs rendered  $\alpha$  exon inclusion. We conclude that, in neural cells, skipping of the  $\alpha$  exon depends on two antagonistic exonic elements located in the flanking constitutive exons.

© 2003 Elsevier B.V. All rights reserved.

**Keywords:** Cis-acting splicing element; Splicing factor; Tight junction; Epithelium; Neural cell

### 1. Introduction

A major mechanism for generation of protein diversity in eukaryotes is the alternative splicing of RNA polymerase II transcripts. This mechanism joins different combinations of 5' and 3' splice sites of a given pre-mRNA in developmentally and cell-specific controlled events [1,2]. Although up to 59% of all genes on a single chromosome are alternatively spliced [3,4], the cues that regulate this process are not fully understood. Recent evidences support the requirement of pre-mRNA sequence elements which may act positively or negatively on splice site recognition and pairing. These may influence competing splicing pathways or are required for cell-specific splicing patterns [5–7]. These elements are intronic (e.g. Refs. [8–12]) or exonic (often in the alternatively spliced exon) (e.g. Refs. [13–17]). In spite of the large amounts of exonic elements described thus far, no consensus sequence can be deduced from them.

However, they function as binding sites for splicing factors such as SR proteins.

Key participants in splice site recognition and selection regulation are the members of the SR (Ser/Arg-rich) family of proteins. These proteins play a role in constitutive and alternative splicing, by binding to exonic splicing enhancers (ESEs) and enhancing or repressing spliceosome assembly at adjacent splice sites. The differential expression of SR proteins and hnRNPs during development and between tissues supports the notion that such expression patterns can affect the alternative splicing of various mRNAs *in vivo* [18–23]. Also, SR proteins are distributed throughout the nucleoplasm and are rapidly redistributed in the nucleus [24] and some of them can shuttle between the nucleus and the cytoplasm [25]. For these reasons, complex alternative splicing regulatory mechanisms should be invoked.

Coordination between the multiple factors and elements is required to carry out a single splicing event (e.g. Refs. [11,13,16,26–33]), and a combination of controlled interactions between the participants involved is not rare [33,34].

\* Corresponding author. Tel.: +52-5061-3954; fax: +52-5747-7083.  
E-mail address: [jvaldes@mail.cinvestav.mx](mailto:jvaldes@mail.cinvestav.mx) (J. Valdés).

The pre-mRNA of the tight junction (TJ) protein ZO-1 has several alternatively spliced exons and potentially could give rise to as many as 30 different ZO-1 isoforms [35]. In most epithelia and endothelia, ZO-1 $\alpha$ <sup>+</sup> and ZO-1 $\alpha$ <sup>-</sup> isoforms are present. These isoforms differ in the presence of the 80-amino-acid-long  $\alpha$  domain, which results from the alternative splicing of the 240-nt  $\alpha$  exon [36]. While endothelia make leaky TJs, epithelia can make both hermetic and leaky TJs [36–40], ensuring vectorial transport across epithelia and preventing paracellular back diffusion [41]. There is a strong correlation of ZO-1 $\alpha$ <sup>+</sup>/ZO-1 $\alpha$ <sup>-</sup> expression ratios to TJ phenotypes. Hermetic TJs with ZO-1 $\alpha$ <sup>+</sup>/ZO-1 $\alpha$ <sup>-</sup> ratios  $\geq 4$  are found in cell cultures and ex vivo tissues composed of epithelial and endothelial cells, whereas leaky TJs with ZO-1 $\alpha$ <sup>+</sup>/ZO-1 $\alpha$ <sup>-</sup> ratios  $\leq 0.9$  are found in most endothelial cell lines and tissues [37,38]. Furthermore, antisense oligonucleotides targeted to the ZO-1 $\alpha$  domain perturb efficient TJ formation and barrier functions in endothelial and epithelial cells [38], suggesting a direct involvement of the  $\alpha$  domain in the modulation of TJ functions.

The cDNAs for ZO-1 from human [42], mouse [43] and dog [35] have been cloned and characterized. This enabled us to clone human and canine genomic fragments coding for the  $\alpha$  exon, partial sequences of the adjacent constitutive exons and the intervening sequences between them. With these tools we focused on understanding the  $\alpha$  exon alternative splicing mechanism. Here we identified and discerned the roles of two exonic cis-acting elements involved in the control of the  $\alpha$  exon inclusion/skipping in vivo, using neural and epithelial cell hosts. These elements were localized in the flanking constitutive exons and do not resemble previously reported cis-acting elements.

## 2. Materials and methods

### 2.1. Cell cultures

MDCK cells (derived from dog kidney epithelia) were cultured in DMEM as described [44]. HeLa, C6 and SH-SY5Y cells were grown in DMEM supplemented with 10% neonate serum, and with 10% fetal calf serum, 2 mM pyruvate and nonessential amino acids (according to directions of the American Type Culture Collection), respectively.

### 2.2. Oligonucleotides

The following primers (all 5'→3') were used for genomic PCR amplification, for RT-PCR, in vivo splicing assays, site directed mutagenesis, and PCR generated run-off transcription DNA substrates. Their correspondent positions in the canine ZO-1 minigene (accession no. AF169195), in the pcDNA3 vector, and in the DUP4-1 plasmid are indicated. *B*: GAGGCTGGTAGGGCTGT-TTGTCATCG; reverse complement (RC) of nt 1740–1765. *B3*: TCATAGCGTGGTCTGCTGTCATAGGAC;

RC of nt 1872–1898. *C2*: GACTCCCCTGGATTAAAA-CAGC; nt 204–226. *C3*: ATGAAGACACAGATACAGAAAGGCGGG; nt 1–26. *44*–: GTTGA-TGATGCTGGGTTTG; RC of nt 612–631. *159*<sup>+</sup>: AAGAACACCAAGCACTGAGG; nt 727–746. *729*–: GCTGCCTCAGTGCTTGGTGTCTT; RC of nt 727–750. *2196*–: GCTTGAGGACTCGTATCTGT; RC of nt 1634–1653 (with a mismatch). *31*<sup>+</sup>: ATATTT-TACCCCTTCACAGAAAGCAGAAGC; nt 549–578. *31*–: RC of primer 31<sup>+</sup>. *52*<sup>+</sup>: GCAAGG-TAAGTGTGCTGCAGTGTTGC; nt 803–829. *52*–: RC of primer 52<sup>+</sup>. *3' int1*<sup>+</sup>: CACTTCACAAAAGCA-GAAGC CTCATC; nt 559–585. *3' int1*–: RC of primer 3' int1<sup>+</sup>. *3' int2*<sup>+</sup>: GTGAATTTTTTACACAAGTGATAGAAA G; nt 1445–1474. *3' int2*–: RC of primer 3' int2<sup>+</sup>. *50E1*: ATCTAGTTCTTGATCAGTGTAGG; RC of nt 38–50. *T7*: AACTAGAGAACCCACTGCTTACTG; nt 827–850 of the pcDNA3 vector. *SP6*: ACGGGG-GAGGGGCAAACAAC; RC of nt 1068–1087 of the pcDNA3 vector. *XD*: GGTCTAGAGTGAACCGTCACAGATCAGC; nt 534–553 of the plasmid DUP4-1. *CD*: CCATCGATAGGCAGAATCCAGATGC; RC of nt 1215–1232 of the plasmid DUP4-1.

### 2.3. DNA isolation, sequencing and computer analyses

Phenol extraction of MDCK cells and cloning procedures in plasmid DNA and restriction analyses were carried out as described [45]. DNA sequencing was performed using the dideoxy chain termination method with the Sequenase™ enzyme as described by the manufacturer. ClustalW alignment and ESE search were performed on-line at <http://www.workbench.sdsc.edu>, and at <http://www.exon.cshl.org/ESE> (Cartegni, L., Zhu, Z., Zhang, M., and Krainer, A. 2000), respectively.

### 2.4. PCR amplification of the $\alpha$ domain genomic environment

Genomic DNA (0.1  $\mu$ g) from MDCK cells was used as template in a PCR reaction with primers C3/B3. These were targeted, respectively, to the coding sequences of the acidic and the proline-rich domains of the canine ZO-1 [35]. The PCR was carried out in the presence of 1.75 mM MgCl<sub>2</sub>, and 2.5 U of Elongase™ Enzyme Mix (Gibco-BRL). Samples were denatured at 95 °C for 5 min, followed by 35 cycles of 1.5 min denaturing step at 95 °C, 3-min annealing step at 55 °C, and 6-min extension step at 65 °C. A single genomic 1898-bp product was amplified, which was analyzed by restriction mapping. Nested PCR of this fragment was carried out with primers C2/B.

### 2.5. Constructs

*Plasmid pNoTA5*: The 1898-bp band amplified by PCR was cloned into the pNoTA/T7 vector (5'→3') following the

instructions of the manufacturer. From the positive candidates, clone pNoTA5 was selected for subcloning procedures and sequencing. The pNoTA5 insert along with part of the flanking polylinker sequences were used for expression purposes. *Plasmid p $\alpha$ AS*: pNoTA5 was digested with *Bam*HI, and the 1898-bp wild-type minigene insert was subcloned in the *Bam*HI site of pcDNA3 expression vector (Invitrogen). *Plasmids pM3ssI1*, *pM5ssI2*, *p $\Delta$ 3' int1*, and *p $\Delta$ 3' int2*: These plasmids were generated utilizing the QuikChange™ Site-Directed Mutagenesis kit (Stratagene) as recommended by the manufacturer. The primers used were 31+/31–, 52+/52–, 3' int1+/3' int1–, and 3' int2+/3' int2–, respectively. In all cases the template was the p $\alpha$ AS plasmid. *Plasmid p $\alpha$ DUP*: The 400-bp *Bst*1107–*Pst*I fragment of p $\alpha$ AS was blunted and subcloned in the blunt-repaired *Apa*I and *Bgl*II sites of the DUP4-1 plasmid (a generous gift of D. Black and E.F. Modafferi). *Plasmid p5' BP*: The 638-bp *Bam*HI–*Hinc*II fragment of p $\alpha$ AS was subcloned into the *Bam*HI, and *Eco*RV sites of the pcDNA3 vector. *Plasmid p3' BP*: The 1250-bp *Hinc*II–*Bam*HI fragment of p $\alpha$ AS was subcloned into the Klenow-blunted *Hind*III site, and *Bam*HI site of the pcDNA3 vector. *Plasmid p $\alpha$  $\Phi$* : The 196-bp *Hae*II fragment of the  $\Phi$ X174 phage was inserted in the *Eco*RV site of pBlueScript KS. The 229-bp *Hind*III–*Bam*HI fragment of this plasmid was linear-ligated to the 584-bp *Xba*I–*Hind*III fragment of the pNoTAh plasmid (the human counterpart of plasmid pNoTA5) so as to rescue the configuration AD exon– $\alpha$  intron—the initial 8-bp of the  $\alpha$  exon, thus reconstructing the initial 13-bp of the  $\alpha$  exon. The resulting 813-bp *Xba*I–*Bam*HI fragment was subcloned in the same sites of pBlueScript KS. This plasmid was cut open with *Bam*HI to insert the 659-bp *Bam*HI–*Bst*YI fragment from pNoTAh, which contained the last 12 bp of the  $\alpha$  exon and part of the PR intron. The *Kpn*I–*Xba*I fragment of this clone (comprising AD exon– $\alpha$  intron– $\Phi$  substituted  $\alpha$  exon, which has the 5' splice site of the PR intron intact) was ligated in the same sites of the pNoTAh. Finally, the whole substituted human minigene, flanked by *Xba*I sites, was subcloned into the same site of the pcDNA3 vector. *Plasmid pCKpn*: The 808-bp *Kpn*I fragment of p $\alpha$ AS was subcloned in the same site of the pcDNA3 vector. *Plasmid p $\Delta$ 80*: The 1818-bp *Hpa*II–*Eco*RV fragment of pNoTA5 was subcloned in the *Eco*RV site of the pcDNA3 vector. *Plasmid p $\Delta$ 35*: The 603-bp *Bcl*I–*Hinc*II fragment was replaced in the *Hind*III and *Hinc*II sites of p $\alpha$ AS. *Plasmid p80S*: The 1818-bp *Hpa*II–*Xba*I fragment was subcloned in the *Sma*I site of pBlueScript KS + vector. The insert of this intermediary was rescued with *Eco*RV and *Xba*I, and subcloned behind a 73-bp fragment comprising exons 6 and 8 of the cDNA of the  $\beta$  subunit of the L-type calcium channel (in the Klenow-repaired *Hind*III site, and the *Xba*I site, respectively). The 5' end of the canine minigene of the later plasmid was rescued with *Kpn*I (harboring the substitution of the initial 80 bp), which was used to replace the *Kpn*I 808-bp fragment of the wild-type minigene in the plasmid p $\alpha$ AS. *Plasmid p $\Delta$ 30SI*: The PCR

product generated with primers C3/50E1 was cloned in the *Hind*III site of the p $\Delta$ 80 plasmid, in reverse orientation. *Plasmid p $\Delta$ X*: The 280-bp *Xho*I fragment was deleted from plasmid p $\alpha$ AS. *Plasmid p $\Delta$ 105*: The 105-bp *Ppu*MI–*Eco*RV fragment was deleted of p $\alpha$ AS. *Plasmid p $\Delta$ H*: The 1527-bp *Hha*I fragment of p $\alpha$ AS was repaired and subcloned into the *Eco*RV site of the pcDNA3 vector. *Plasmid p $\Delta$ PDE*: To eliminate the 87 bp between the *Bst*EII and *Xho*I sites of the PD exon, the 300-bp *Xho*I fragment of the p $\alpha$ AS construct was repaired and inserted in the *Bst*EII

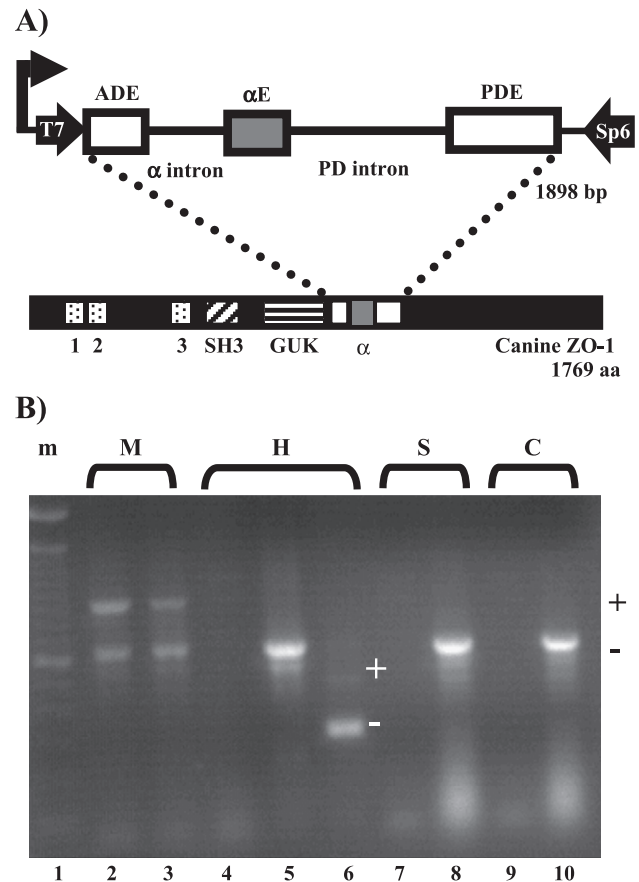


Fig. 1. In vivo splicing of the ZO-1  $\alpha$ AS minigene transcripts. (A) Schematic representation of the p $\alpha$ AS minigene construct, drawn to scale. White boxes represent the acidic domain (AD), and proline-rich domain (PD) exons. The gray box indicates the  $\alpha$  domain exon ( $\alpha$  exon). The thin lines represent the  $\alpha$ , and PD introns. T7 and SP6 arrows, respective phage transcription start sites. The thick arrow indicates the CMV transcription start site. As a reference, the coding domains of the canine ZO-1 cDNA appear underneath. Dotted boxes, PDZ domains; crosshatched box, SH3 domain; and hatched box, Guanylate kinase, GUK, domain. (B) MDCK (M), HeLa (H), SH-SY5Y (S) and C6 (C) cells were transfected with the p $\alpha$ AS plasmid. RT-PCR reactions were carried out 48 h post-transfection. Using the set of primers C3/B3, the amplified products (lanes 1–5, 8, and 10) corresponded to the  $\alpha$ + (+; 913 bp) and/or the  $\alpha$ – (–; 673 bp) transcripts. Mock-transfected HeLa cells rendered no products (lane 4). In nested PCR experiments, using primers C2/B, this cell line yielded  $\alpha$ + (576 bp) and  $\alpha$ – (336 bp) transcripts. The neural cell lines lacked the specific  $\alpha$ + expected product (280 bp), when monitored with the C3/44– primers (lanes 7, and 9). As a positive control, the mRNA of untransfected MDCK cells was used (lane 2). Lane 1 (m), 100-bp ladder (Gibco-BRL).

and *XhoI* repaired sites of the *pcαAS* plasmid. *Plasmid pXglo*: The Klenow-blunted PCR product of DUP4-1, using primers XD/CD, was inserted in the Mung Bean blunted PpuMI site of *pcαAS*. *Plasmid pXΔ100*: The 100-bp *HindIII*–*AvaII* fragment was deleted from *pΔX*. *Plasmids pΔ35ΔX* and *pΔ80ΔX*: The 280-bp *XhoI* fragment was deleted from plasmids *pΔ35* and *pΔ80*, respectively.

## 2.6. Transfection and RT-PCR analyses

RT-PCR analyses for *in vivo* splicing reactions of the ZO-1 minigene constructs were carried out as follows. All expression constructs were transfected into epithelial (HeLa and MDCK), and neural (SH-SY5Y and C6) cells using the LipofectAmine Plus™ Reagent (Gibco-BRL) according to the instructions of the manufacturer. Transfection efficiencies were greater than 90% as monitored with a Lac-Z reporter plasmid. Total RNA was purified from the cultures as described [46], 48 h post-transfection, and contaminant DNA was eliminated with RNase-free DNase I as described [47]. Splicing products of the constructs were revealed using the SuperScript™ One-Step RT-PCR System (Gibco-BRL), suitable PCR conditions and the appropriate set of primers (as indicated in each figure), according to the manufacturer. In most reactions, one of the primers was

targeted to the vector, to monitor the transcripts of the transfected clones. For this reason, some PCR products are larger than the length of the  $\alpha$  exon, and vary among different constructs because most of the deletions are internal with respect to the target sites of the primers. In all cases, minus RT reactions were analyzed (e.g. Fig. 5). Since large amounts of unspliced precursors were obtained, the relative amounts of PCR products were estimated by comparison with  $\beta$ -globin pre-mRNA amplified in parallel (e.g. Figs. 5 and 6). Typical results from SH-SY5Y and HeLa cell cultures are shown. The identity of the PCR products was verified by restriction analysis or sequence analyses, or both. Our RT-PCR results were also performed with total RNA purified with phenol-free RNA purification procedures (Micro-to-Midi Total RNA Purification System; Invitrogen). We found no differences between both methods (e.g. Figs. 6 and 8). RT analyses for BPS identification were carried out with 30  $\mu$ g of total RNA from transfected cells or with the whole *in vitro* splicing reactions. Primers used were 2196 – for the PD intron, and 44 – for the  $\alpha$  intron. Primers (0.5  $\mu$ g) were labeled with 50  $\mu$ Ci [ $^{32}$ P]-dATP (NEN Life Science) and 25 U of T4 Polynucleotide Kinase (Boehringer) as recommended by the supplier, for 0.5 h at 37 °C. RT reactions contained  $3 \times 10^5$  dpm of labeled primers, 10 mM DTT, 0.5 mM each dNTP (Sigma), 0.25 U RNasin, 3

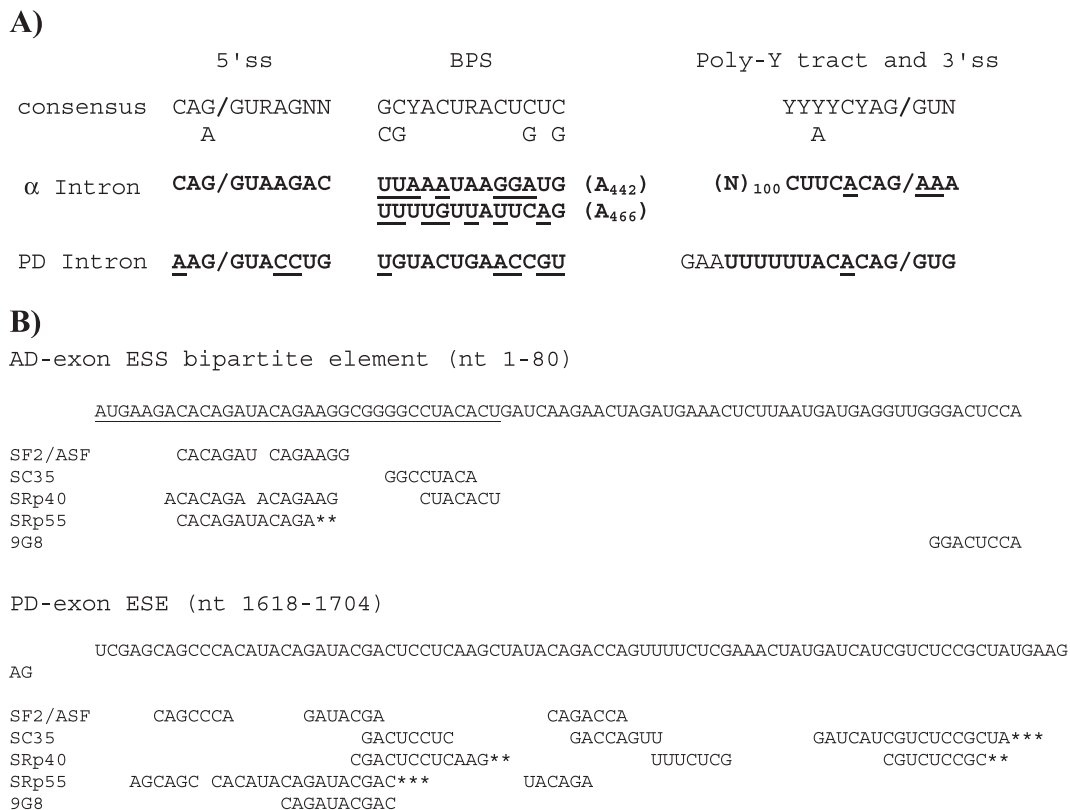


Fig. 2. Intronic and exonic cis-acting elements of the  $\alpha$ AS minigene. (A) Comparison of the 5' splice sites, the 3' splice sites, Branch Point Sequences and poly-pyrimidine tracts of the ZO-1 minigene with consensus. Nucleotides not corresponding to consensus are underlined. (B) Putative binding sites of different SR proteins (SF2/ASF, SC35, SRp40, SRp55 and 9G8) found within the ESS and ESE elements of the ZO-1 minigene. The negative regulator of the ESS appears underlined. The search was done with the ESE finder program (v1.1). In some cases, two (\*\*) or three (\*\*\*) overlapping sites were found.

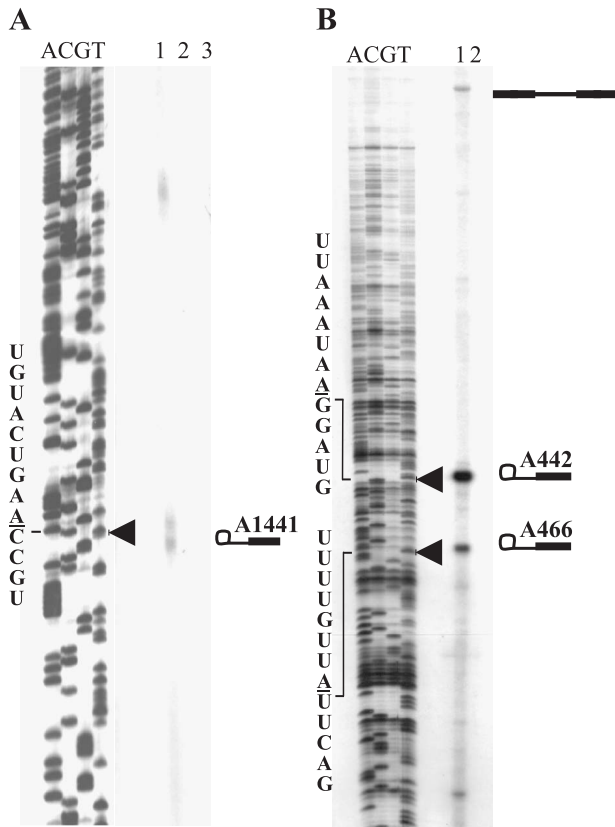


Fig. 3. Identification of functional branchpoint sequences (BPSs). Primer extension analysis was carried out to detect the functional BPSs involved in the splicing of the  $\alpha$  exon. (A) One strong sequence is the functional BPS for PD intron. MDCK cells were transfected with the plasmid p $\Delta 3'$  SSINT-2. Forty-eight hours later, RNA was obtained and primer extension was carried out. Transfected cells yielded two stop signals (at nt 212, and nt 213) and a read-through product (lane 1). Negative controls were non-transfected cells and yeast tRNA (lanes 2 and 3, respectively). Sequencing reaction was carried out with the same primer (2196 –) to identify the functional BPS. (B) Run-off transcripts from the T7 promoter of plasmid p $\Delta 3'$ SSINT-1 were incubated in HeLa nuclear extracts prior to primer extension analysis. Two stop signals and a read-through product were detected (at nt 193, and nt 169; lane 1) for the  $\alpha$  intron. No signals were detected in the yeast tRNA negative control (lane 2). Sequencing reaction was carried out with the same primer (44 –). Stop signals (arrowheads) and unspliced precursors are shown to the right. The sequences of the BPSs appear to the left.

mM sodium phosphate, 40  $\mu$ g/ml Actinomycin D and 20 U SuperscriptII™ (Gibco) enzyme, in the enzyme buffer, and were incubated for 2.5 h at 42 °C. Annealing was carried out at  $T_m - 5$  °C for 0.5 h. Total RNA from mock transfected cells and 10  $\mu$ g of yeast tRNA were used as controls. Reactions were stopped with 1  $\mu$ l of 0.5 M EDTA and 0.5  $\mu$ g each RNases A and T1. After phenol extraction and ethanol precipitation, extended products were electrophoresed on the side of sequence reactions carried out with the same primers. In vitro splicing reactions were set with 5 ng of synthetic transcripts and 50  $\mu$ g of HeLa nuclear extracts (Gibco-BRL) in the RNA Splicing System (Promega) as recommended by the manufacturer. Reactions were incu-

bated for 2 h at 30 °C. Products were phenol-extracted and ethanol-precipitated prior to use in the RT reactions.

### 2.7. Synthetic transcripts

For the  $\alpha$  intron BPS identification, 1  $\mu$ g of *Kpn*I-digested plasmid p $\Delta 3'$  int1 was used as template. Run-off transcripts were synthesized with the Riboprobe System T7 (Promega), as recommended by the manufacturer, in the presence of a fourfold molar excess of the m<sup>7</sup>G(5')ppp(5')G CAP analog.

## 3. Results

### 3.1. The $\alpha$ exon is skipped in non-epithelial cell lines

Fig. 1A depicts the pc $\alpha$ AS minigene construct used in this work. In agreement with the canine ZO-I cDNA [35], it contains part of the acidic domain (AD exon, 236 bp), the  $\alpha$  domain ( $\alpha$  exon, 240 bp), part of the proline-rich domain (PD exon, 437 bp), and two intervening sequences (GenBank accession no. AF169195). The  $\alpha$  intron and the PD intron were 332 and 653 bp, respectively. In Fig. 2A, the 5' and 3' splice sites of both introns were compared with canonical splice sites. The 5' ss of the  $\alpha$  intron and the 3' ss of the PD intron were canonical. The latter with a poly-pyrimidine tract (U<sub>6</sub> stretch) 6 nt upstream from the 3' ss. The remaining splice sites were not canonical. Assuming that the AD and PD exons are constitutively recognized—probably

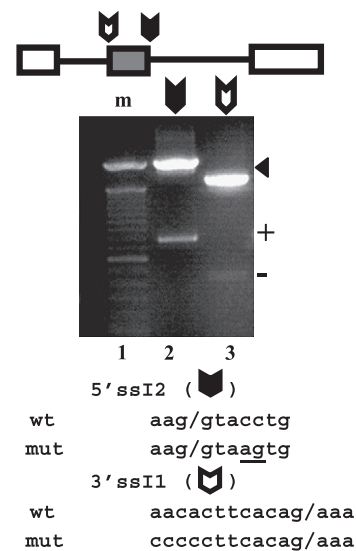


Fig. 4. The  $\alpha$  exon is flanked by weak 3' and 5' splice sites. The 3' splice site (p3' SSII, solid arrow) and the 5' splice site (p5' SSII, open arrow) flanking  $\alpha$  exon were mutated to consensus (top and bottom), and the effect was analyzed using in vivo RT-PCR splicing assays in SH-SY5Y cells (mid section). Lane m, 100-bp DNA ladder. Arrowheads, unspliced precursors (bands of 1734 and 1654 bp, respectively). +,  $\alpha$ + transcripts (749-bp band). –,  $\alpha$ – transcripts (429-bp band). The wild-type (wt) and mutated (mut; underlined) splice sites are shown. PCR primers were: T7/2196 – for p5' SSII; C3/2196 – for p3' SSII.

because they have good exon recognition elements and/or good interactions between 5' ss and 3' ss binding factors and polyadenylation factors—it is possible that the  $\alpha$  exon inclusion might be subject to negative regulation in non-epithelial cells. This assumption agrees with the early ZO-1 $\alpha^-$  expression (8-cell stage) and late ZO-1 $\alpha^+$  expression (32-cell stage) during mouse development [48]. Also, this suggests that for the  $\alpha$  exon inclusion, auxiliary factors might be required in addition to the basal splicing machinery. Such factors could be involved in the recognition of the  $\alpha$  exon–intron boundaries. To explore these possibilities, we focused on the identification of cis-acting elements involved in the alternative splicing of the  $\alpha$  exon in the p $\alpha$ AS minigene.

In vivo splicing reactions in different cell lines were carried out. Non-transfected MDCK cells rendered a 5:1 ratio of  $\alpha^+/\alpha^-$  products (Fig. 1B, lane 2). This ratio was somewhat modified when the p $\alpha$ AS construct was transfected to this cell line (Fig. 1B, lane 3). Possibly, the overexpressed minigene competed for the splicing machinery. In transfected epithelial HeLa cells, the main product was  $\alpha^-$  (Fig. 1B, lane 5), and nested PCR of the same reaction mix revealed that the  $\alpha^+$  product was present also, although to a lesser extent (Fig. 1B, lane 6). No ZO-1 transcripts were detected in mock-transfected HeLa cells (Fig. 1B, lane 4), because of the low ZO-1 expression in this cell line. The p $\alpha$ AS construct was tested also in SH-SY5Y and C6 (neural) cells, because they do not express ZO-1 and

may lack epithelial-enriched trans-acting factors. In these cell lines  $\alpha^-$  products were detected only (Fig. 1B, lanes 8 and 10, respectively), and no  $\alpha^+$  products were obtained in nested PCR experiments (Fig. 1B, lanes 7 and 9, respectively). These results reflect the actual expression of the ZO-1 alternative splicing in epithelial cells (and what was expected from cell lines devoid of ZO-1), and suggested a possible enrichment of the splicing auxiliary factors in epithelial cells.

Two putative BPSs in the  $\alpha$  intron and one in the PD intron were identified (Fig. 2A) when compared to others previously reported [49–51]. To search for the functional BPSs, inactive 3' splice sites p $\alpha$ SA derivatives of both introns were generated. The PD intron BPS was identified by transfection of the p $\Delta$ 3' int2 construct into HeLa cells, followed by primer extension analysis. As expected, the extended product ended in an A residue (nt 1441 of  $\alpha$ AS), 20 bp upstream from the 3' ss (Fig. 3A) in a nearly canonical BPS, UGUACUGA4CCGU. An additional contiguous A also rendered a stop signal, probably due to a bypass effect of the primer extension analysis. For the  $\alpha$  intron BPSs, the p $\Delta$ 3' int1 construct was also tested in vivo but we were not able to detect any signal from these assays (not shown). Therefore, synthetic transcripts of the p $\Delta$ 3' int1 derivative were incubated in HeLa nuclear extracts prior to primer extension analysis. These reactions showed that two A residues (nt 442 and nt 466 of  $\alpha$ AS), at 127 and 103 nt from the 3' ss, might be

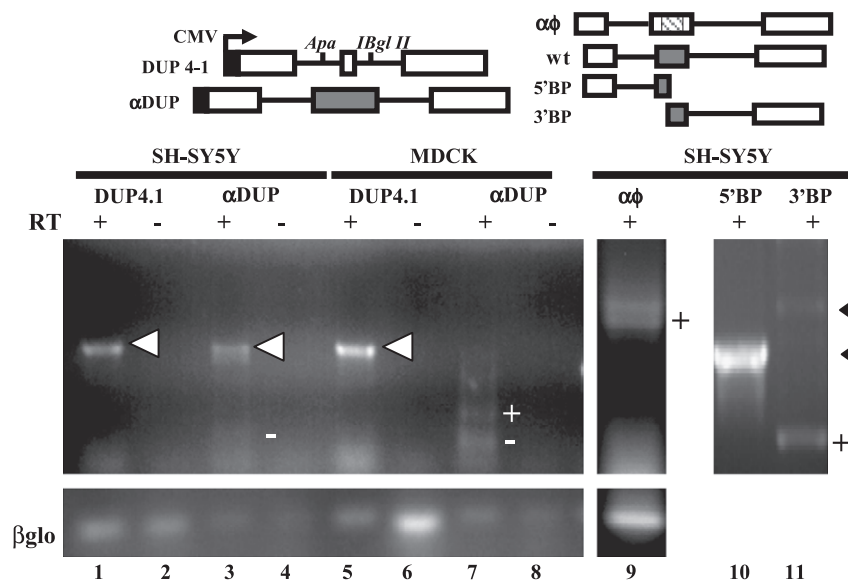


Fig. 5. The  $\alpha$  exon does not contain elements involved in its alternative splicing. Top: In the construct p $\alpha$ DUP, the  $\alpha$  exon replaced the mini-exon of the DUP 4-1 plasmid [10]. The  $\alpha$  exon was replaced with non-related sequences in the p $\alpha$  $\Phi$  construct. The p $\alpha$ AS construct was split in two, giving rise to the p5' BP and p3' BP constructs. Bottom: In neural (SY-SY5Y) and epithelial (MDCK) cells, the DUP4-1 construct (lanes 1, 2, 5, and 6) rendered unspliced precursors (bands of 804 bp), whereas the p $\alpha$ DUP construct (lanes 3, 4, 7, and 8) rendered  $\alpha^-$  transcripts (bands of 328 bp). This latter construct also rendered  $\alpha^+$  transcripts in MDCK cells (band of 568 bp). The remaining constructs were tested in neural cells only. The p $\alpha$  $\Phi$  construct (lane 9) yielded  $\alpha$ -replaced  $\Phi$  transcripts (band of 995 bp). The unspliced precursors of the constructs p5' BP, and p3' BP were 715 and 926 bp, respectively (lanes 10 and 11). The  $\alpha^+$  product obtained from construct p3' BP was 273 bp. PCR primers were: XD/CD for DUP4-1 and p $\alpha$ DUP; T7/SP6 for p $\alpha$  $\Phi$ ; T7/44 – for p5' BP; 159+/2196 – for p3' BP. Arrowheads indicate unspliced precursors; + and – indicate the  $\alpha^+$  and  $\alpha^-$  transcripts. RT+ and RT– indicate the presence or absence of reverse transcriptase in the reactions. The transcripts of the  $\beta$  globin input controls are shown.

utilized as BPSs in vitro (Fig. 3B). These BPSs are far from canonical, UUAAAUAAGGAUG and UUUUGUUU UUCAG, respectively. The A466 residue is utilized 5–10-fold less efficiently than the A442 residue. Surprisingly, no clear poly-Y tract is around these residues. A stretch of eight uridines was located 5 bp upstream the A442 and a poly-Y-rich sequence of 25 nt (including the A466 residue) is located 10 bp downstream the A442. Although any of the putative poly-Y tracts might be functional for both BPSs detected, it must be noted that none of them resemble typical poly-Y tracts.

The weak splice sites flanking the  $\alpha$  exon were analyzed in a similar way as those of the fibronectin exon EIIIB [26]. The 3' ss of the  $\alpha$  intron and the 5' ss of the PD intron were replaced with stronger splice sites, then we monitored the  $\alpha$  exon inclusion in SH-SY5Y cells. Albeit most of the products observed were unspliced precursors, the PD intron 5' ss mutant (Fig. 4, lane 2) was efficiently recognized as a strong splice site by the cell's splicing machinery. In contrast, the  $\alpha$  intron 3' ss mutant (actually a strengthened poly-Y tract mutant) was not recognized as such (Fig. 4, lane 3), probably because the branch point sequences of this intron were located farther upstream.

Whether the  $\alpha$  exon contained cis-elements that promoted its alternative splicing in a non-epithelial background was also explored in SH-SY5Y cells. The  $\alpha$  exon, along with 54 bp of the adjacent  $\alpha$  intron and 10 bp of the adjacent PD intron, was inserted in a foreign minigene construct,  $\beta$ -globin (DUP4-1). Like the 7-nt mini-exon of the troponin I gene that behaves in different cell lines [52], the DUP4-1 construct rendered unspliced precursors (Fig. 5, lane 1), because in order to include this minixon at least 177 bp of intronic enhancer sequences is required [10]. The  $\alpha$ DUP construct rendered  $\alpha$  – products in neural cells (Fig. 5, lane 3), and both  $\alpha$ + and  $\alpha$  – products in MDCK cells (Fig. 5, lane 7). This suggested that, in an epithelial context, the  $\alpha$  exon or the flanking intronic sequences (ca. 100 bp upstream and 15 bp downstream of the  $\alpha$  exon) might contain exon inclusion control elements. Therefore, most of the  $\alpha$  exon sequences were substituted with non-related phage sequences, keeping 13 and 12 nt of the flanking wild-type 3' and 5' splice sites. The  $\alpha\Phi$  substituted exon was included by the neural cells' splicing machinery (Fig. 5, lane 9), suggesting that some intronic sequences might be playing a role in the  $\alpha$  exon inclusion process. Taken together, our results reflect the difference in strength of the 3' splice sites of both introns, the apparent preferential distal 3' splice site selection in neural cells, and the possible need of epithelial-enriched factors for  $\alpha$  exon inclusion. They also suggest that the  $\alpha$  exon lacks cis-acting elements that control its alternative splicing, and that recognition of the adjacent 3' ss and 5' ss (and other intronic sequences) by trans-factors suffices to carry out the inclusion process. Therefore, we first searched for splicing enhancer/silencer elements outside of the  $\alpha$  exon.

### 3.2. Two exonic elements in the flanking constitutive exons are involved in $\alpha$ exon inclusion/skipping

The  $\alpha$ AS minigene was analyzed with the ESE finder program to search for repeated hexamer-like patterns or elements relevant for  $\alpha$  exon alternative splicing. Fig. 2B and Table 1 show all putative motifs found within the  $\alpha$ AS minigene, including binding sites for SR proteins. Many of these motifs were not exact matches with the reported sequences and none of them have been directly tested to be involved in this process. To disclose any possible functionally active cis element, deletion derivatives of the p $\alpha$ AS construct and in vivo splicing assays were carried out.

From the p5'BP construct (AD exon– $\alpha$  intron–68 bp of the  $\alpha$  exon), only unspliced precursors were obtained (Fig. 5, lane 10), suggesting either that the AD exon might contain an exonic splicing silencer (ESS), or a more complex  $\alpha$  intron splicing control. The p3'BP derivative (172 bp of the  $\alpha$  exon–PD intron–PD exon) rendered  $\alpha$  exon–PDE spliced products (Fig. 5, lane 11), suggesting that PD exon might contain an ESE. These findings support the notion that, although not fully evident, the first intron might contain negative elements affecting this splicing mechanism.

Deletions at the 5' end of p $\alpha$ AS defined the putative ESS in the AD exon. The neural cells transfected with the

Table 1  
Putative cis-acting elements found in the canine  $\alpha$ AS

Sequence	System	Reference	Position in $\alpha$ AS <sup>a</sup>
UGCAUG	EIIIB Fibronectin	[8]	968
	<i>c-src</i>	[10]	
UCBBCRAUCAAC	<i>Dsx</i>	[75]	178
			603
CAGGUAAGAC	CT/CGRP	[9]	234
BGGG	$\beta$ -Tropomyosin	[76]	71
			512
			675
			910
			1017
			1346
			1539
			1836
AGUGCUGUGU	Myosin heavy chain	[77]	635
AGUGCUGUGU	( <i>Drosophila</i> )		1102
			1525
CAACGACGA	<i>Drosophila</i> RSF1	[78]	178
AAACGCGCG			603
TGC <sub>(n)</sub> YYYY	Actinin	[55]	816
GAAR-type	Caldesmon	[14]	1699
			1720
			1819
			1855
	Troponin-T	[15]	1486
	tat-rev exon HIV	[16]	308
	<i>c-src</i>	[33]	1486

B = A or U; R = purine; Y = pyrimidine.

<sup>a</sup> Sequence hits found in  $\alpha$ AS were not always identical.

construct pCKpn (AD exon- $\alpha$  intron- $\alpha$  exon) rendered unspliced products only (Fig. 6, lane 2). Upon deletion of the initial 80 bp of the AD exon, we observed  $\alpha^+$  and  $\alpha^-$  transcripts also (Fig. 6, lane 4), whereas deletion of the first 35 bp resulted in  $\alpha^+$  and unspliced transcripts (Fig. 6, lane 3). To test this ESS element, corresponding substitution and inversion constructs were made. In construct p80S the ESS was replaced with different exons, resulting in the rescue of  $\alpha^-$ , unspliced and minute amounts of  $\alpha^+$  products (Fig. 6, lane 6); sequence analysis revealed that such  $\alpha^+$  products were originated from an upstream cryptic splice site. In the p $\Delta$ 30SI clone, the initial 45 bp of the ESS was cloned in reverse orientation. This resulted in the inclusion of the  $\alpha$  exon as well (Fig. 6, lane 5). Altogether, this suggested that the ESS is a bipartite regulator of the  $\alpha$  exon. The initial 35 nt acts proximally as a negative regulator, and the remaining 45 nt acts as a distal positive regulator. This configuration, although localized in the flanking AD exon, resembled the one present in the EDA exon [27].

The minimal sequence of the putative ESE was localized in the middle of the PD exon. Deletion of the distal 280 bp

of pc $\alpha$ AS (p $\Delta$ X) resulted in unspliced precursors only (Fig. 6, lane 7). In contrast, deletion of the terminal 105 bp (construct p $\Delta$ 105) resulted in  $\alpha$  exon skipping (Fig. 6, lane 8). Deletion of the initial 177 bp and the last 194 bp of pc $\alpha$ AS (construct p $\Delta$ H) allowed the rescue of  $\alpha^-$  and  $\alpha^+$  transcripts (Fig. 6, lane 9). Elimination of PD exon sequences other than the ESE in construct p $\Delta$ PDE did not render different products compared to the wild-type construct (Fig. 6, lane 10). Therefore, the putative ESE resides in the *Xho*I-*Hha*I 83-bp fragment of the PD exon. Insertion of the whole  $\beta$ -globin minigene in front of the ESE resulted in transcripts where  $\alpha$  exon was always spliced to the interrupted PD exon. Some of these transcripts have not eliminated all the  $\beta$ -globin introns (Fig. 6, lane 11). Apparently, this ESE is facilitating distal 5' ss recognition and it may function proximally, although inefficiently, in the absence of the putative ESS (as was observed with the p $\Delta$ H construct).

These ESS and ESE that appear to be involved in the alternative splicing of the c $\alpha$ AS minigene reside outside of the  $\alpha$  exon and differ in character from others reported previously, but resemble the configuration that controls the

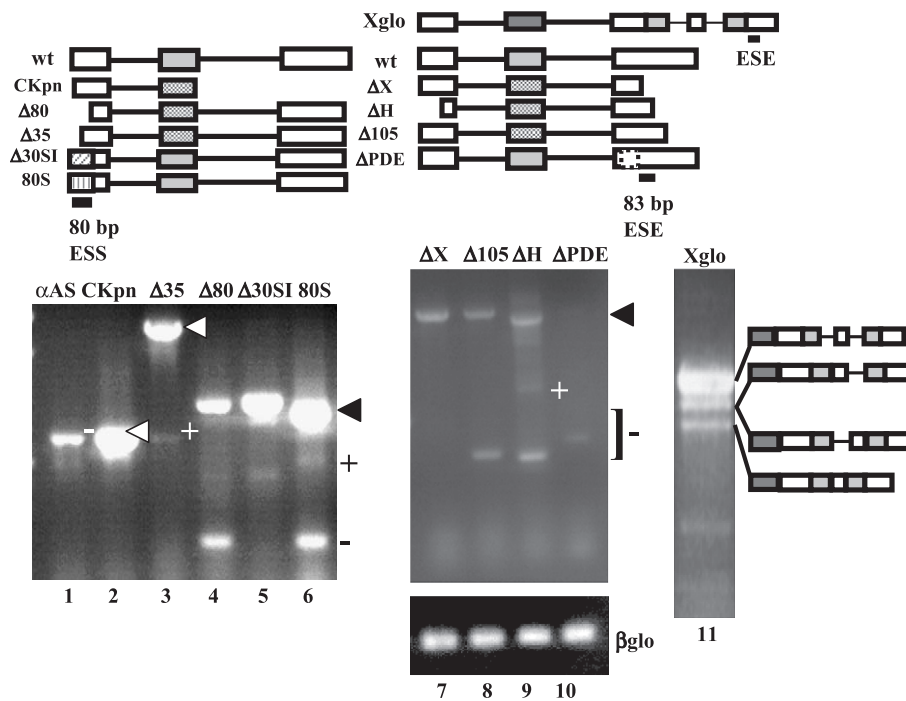


Fig. 6. Two exonic elements antagonistically regulate the  $\alpha$  exon skipping. To limit the minimal sequences of the ESS localized in the AD exon and the ESE localized in the PD exon, several pc $\alpha$ AS deletion derivatives were made (top) and were tested by in vivo RT-PCR splicing assays in SH-SY5Y cells (bottom). Unspliced precursors were obtained with constructs pCKpn (lane 2, band of 715 bp) and p $\Delta$ X (lane 7, band of 1734). With the construct p $\Delta$ H (lane 9), in addition to unspliced precursors (band of 1598 bp),  $\alpha^+$  (band of 613 bp) and  $\alpha^-$  (band of 373 bp) transcripts were observed. The constructs p $\Delta$ 35 and p $\Delta$ 80 (lanes 3 and 4) yielded unspliced precursors (bands of 1735 and 926 bp) and  $\alpha^+$  transcripts (bands of 710, and 273 bp). The p $\Delta$ 105 derivative (lane 8) rendered  $\alpha^-$  transcripts and the unspliced precursor. To test the ESS element, constructs p $\Delta$ 30SI and p80S were made (lanes 5 and 6). In the former, the initial part of the ESS was inverted, which rendered unspliced precursors and  $\alpha^+$  products. In the clone p80S, the ESS was replaced with other exonic sequences. This construct yielded unspliced precursors, and  $\alpha^+$  and  $\alpha^-$  transcripts. The ESE element was further tested by deleting 82 bp in front of the ESE (construct p $\Delta$ PDE, lane 10) and by inserting the whole DUP4-1 minigene in front of the ESE (construct pXglo, lane 11). The p $\Delta$ PDE construct rendered unspliced and  $\alpha^-$  transcripts, whereas the pXglo construct rendered transcripts in which one, two or all introns upstream of the ESE were eliminated (bands of 1381, 1250, 1240 and 1117 bp). The pc $\alpha$ AS control (lane 1) rendered  $\alpha^-$  transcripts (753-bp band). PCR primers were: T7/B3 for pc $\alpha$ AS; T7/44 – for pCKpn; T7/2196 – for p $\Delta$ 35, p $\Delta$ 105, p $\Delta$ H, and p $\Delta$ PDE; C2/2196 – for p $\Delta$ 80 and p80S; T7/729 – for p $\Delta$ 30SI; C3/SP6 for p $\Delta$ X; 159+/SP6 for pXglo. Arrowheads indicate unspliced precursors; + and – indicate the  $\alpha^+$  and  $\alpha^-$  transcripts. The transcripts of the  $\beta$  globin input controls are shown.

alternative splicing of the fibroblast growth factor receptor 2 alternative exon [53]. Coincidentally, several potential binding sites for SR proteins were located within the ESS and ESE elements (Fig. 2B).

3.3. A possible mechanism of action of the ESS and ESE

The presence of partially spliced precursors suggested that the first event in  $\alpha$  exon inclusion could be the elimination of the PD intron and, more importantly, that an intact ESS element is required for appropriate  $\alpha$  exon inclusion/skipping. Fig. 7 shows that partially spliced precursors were obtained with constructs which lacked one (p $\Delta$ H) or both (pX $\Delta$ 100 and p $\Delta$ 80 $\Delta$ X) ESS and ESE elements, or lacked the repressor component of the ESS (p $\Delta$ 35 $\Delta$ X). In the products from these constructs the  $\alpha$  intron was not eliminated, suggesting a cross-talk between the activator of the ESS with the ESE to carry out  $\alpha$  exon–PD exon fusion. Also, the repressor portion of the ESS appears to act proximally towards the 3' ss of the  $\alpha$  intron.

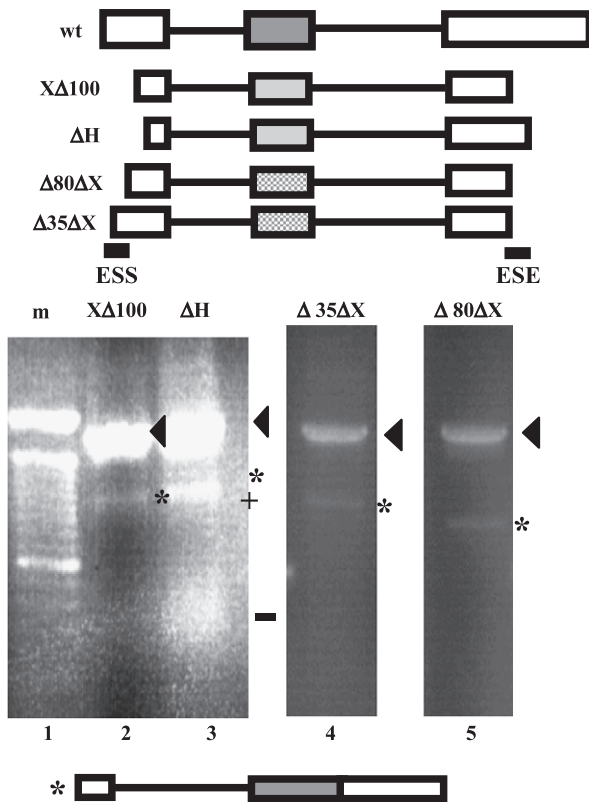


Fig. 7. Partially spliced intermediaries. The constructs pX $\Delta$ 100 (lane 2), p $\Delta$ 35 $\Delta$ X (lane 4) and p $\Delta$ 80 $\Delta$ X (lane 5) rendered unspliced precursors (bands of 1675, 1779 and 1734 bp, respectively), and partially spliced intermediaries (bands of 1122, 1126, and 1081 bp, respectively). In the p $\Delta$ H control (lane 3), the unspliced precursor (1750 bp), the intermediary (1122 bp), the  $\alpha$ + (co-migrating with the 1122-bp band) and the  $\alpha$ - (340 bp) transcripts were observed. Lane 1, 100-bp ladder. Primers were: T7/2196 – for pX $\Delta$ 100 and p $\Delta$ H; T7/SP6 for p $\Delta$ 35 $\Delta$ X and p $\Delta$ 80 $\Delta$ X. Arrowheads indicate unspliced precursors; + and – indicate the  $\alpha$ + and  $\alpha$ - transcripts; \* indicates the partially spliced intermediary.

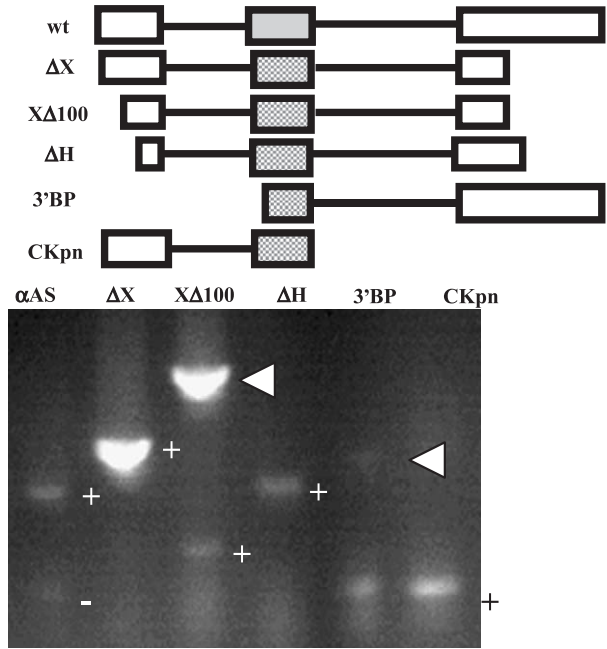


Fig. 8. The functions of the ESE and ESS are bypassed in epithelial cells. Representative clones were transfected into MDCK (epithelial) cells. Plasmids p $\Delta$ X (lane 2) and pCKpn (lane 6) rendered  $\alpha$ + products (bands of 749 and 383 bp, respectively). These plasmids yielded unspliced precursors when transfected into neural cells. As expected, plasmids pX $\Delta$ 100 (lane 3), p $\Delta$ H (lane 4), and p3'BP (lane 5) also rendered  $\alpha$ + products (bands of 417, 613, and 273 bp, respectively). For pX $\Delta$ 100 and p3'BP, unspliced precursors were also obtained (bands of 1070 and 826 bp, respectively). The p $\alpha$ AS positive control yielded both  $\alpha$ + and  $\alpha$ - transcripts (bands of 669 and 429 bp). PCR primers used were: C3/2196 – for p $\alpha$ AS; C3/SP6 for p $\Delta$ X; 159+/SP6 for pX $\Delta$ 100; T7/2196 – for p $\Delta$ H; 159+/2196 – for p3'BP; and T7/44 – for pCKpn. Arrowheads indicate unspliced precursors; + and – indicate the  $\alpha$ + and  $\alpha$ - transcripts.

The effect of this repressor seems to be stronger than the coordinated action of both activators. It is possible that the  $\alpha$  exon–PD exon fusion is required to overcome the function of the repressor, probably by facilitating the recognition of the weak 3' ss of the  $\alpha$  intron or by shortening the distance between both activators. Finally, these data are in agreement with the requirement of an intact ESS element for an adequate control of the alternative splicing of the  $\alpha$  exon.

3.4. The  $\alpha$  exon inclusion is predominant in epithelial cells

Since the  $\alpha$ + transcripts were obtained in transfected epithelial cell lines only, it is possible that redundant auxiliary splicing factors could recognize the various elements in nascent  $\alpha$ AS transcripts, even when some of them are deleted. Examples of all p $\alpha$ AS derivatives that were tested in epithelial MDCK cells are shown in Fig. 8. In contrast to neural cells, constructs p $\Delta$ X and pCKpn rendered  $\alpha$ + transcripts (lanes 2, and 6, respectively). As expected, the positive control constructs pX $\Delta$ 100, p $\Delta$ H, and p3'BP yielded  $\alpha$ + products (lanes 3, 4 and 5, respectively). An explanation for these results is that some splice site-binding, ESE-binding, ESS-binding and bridging fac-

tors, which are capable to carry out their functions in a two- or three-exon systems, might be enriched in epithelial cell lines. These results also showed the otherwise unobserved capacity of all minigene derivative constructs to undergo splicing.

#### 4. Discussion

In this work we studied the alternative splicing of the  $\alpha$  exon in a minigene system of ZO-1 pre-mRNA by means of *in vivo* splicing analyses in cell lines devoid of ZO-1 expression. Two antagonistic exonic elements, ESS and ESE, appear to control the alternative splicing process. Notably, such elements were localized in the constitutive flanking exons rather than in the  $\alpha$  exon itself. Skipping of the  $\alpha$  exon was preferred in non-epithelial cell lines with few or no epithelial-enriched auxiliary splicing factors.

Sequence and functional data of the  $\alpha$ SA minigene revealed that the  $\alpha$  exon is flanked by weak splice sites, whereas strong splice sites flank the adjacent constitutive exons. Although a single mutation strengthened the 5' splice site of the PD intron, a synthetic poly-Y tract did not result in better recognition of the 3' splice site of the  $\alpha$  intron. Partially spliced intermediaries containing the  $\alpha$  intron were rescued as well.

While the BPS of the PD intron was identified at an appropriate distance of the 3' splice site, the  $\alpha$  intron non-canonical BPSs were localized far from the 3' splice site, and had undefined poly-Y tracts. It is possible that the pyrimidine-rich tract downstream from the main  $\alpha$  intron BPS (A442) might function as a bona fide poly-Y tract. The poly-U stretch upstream of this BPS could be utilized instead, in a similar fashion as has been reported for the 59-nucleotide intron of the *Drosophila* mle gene [54]. This possibility must be taken cautiously because there is no conservation in sequence and intron length between the two systems. In this respect, the  $\alpha$  intron of the ZO-1 minigene is more similar with the  $\alpha$ -actinin SM intron. PTB-mediated steric repression of the SM exon in non-SM cells and extracts has been reported [55]. When PTB binds to TCTT motifs [56] located just 54 bp away from the NM 5' splice site, it competes U1 binding [55]. Three TCTT motifs were detected just 30 nt upstream of A442 but we have not critically tested PTB-mediated  $\alpha$  exon inclusion steric repression. Such repression could occur in the  $\alpha$ AS system in a different way as observed for the  $\alpha$ -actinin system. Another possibility is that PTB, and other epithelial cell factors, might be defining the branch point sequence to be utilized as has been suggested before [57], selecting the same 3' splice site regardless of the distance between them [1].

We propose that the strengths of the splice sites of our minigene are: the  $\alpha$  intron 5' splice site  $\cong$  the PD intron 3' splice site > the PD intron 5' splice site > the  $\alpha$  intron 3' splice site. This is based on three observations: first, the sequence complementarity between the U1 snRNA and the AD exon and the  $\alpha$  exon [58,59]; second, the features of the BPSs and poly-pyrimidine tracts

of the  $\alpha$  and PD introns [1,51]; and third, our functional data, in particular, the ease in which the  $\alpha$  exon is spliced to the PD exon.

Apart from the flanking 3' and 5' splice sites, no functional elements within the  $\alpha$  exon were found to participate in the alternative splicing of our system. We are currently trying to identify one or more intronic elements around the  $\alpha$  exon that appear to participate in the regulation of this alternative splicing mechanism.

From the analysis of deletion derivatives we identified two exonic splicing regulating elements, an ESS and an ESE, both located in the flanking constitutive exons. These findings contrast with previous reports on alternatively spliced exons. An exonic silencer, located in the EDA exon, regulates the EDA exon skipping of the human fibronectin mRNA [60], and a 38-bp ESE, located in the exon II, favors the inclusion of the exon II in the protein kinase C  $\beta$ -II mRNA [61]. Nevertheless, the function of the ESS and ESE elements here identified resembles previously reported systems which are controlled by multiple, although intronic, elements [53]. In addition, our ESS and ESE contain several possible binding sites for the SR proteins SF2/ASF, SC35, SRp55, SRp40, and 9G8. SF2/ASF is involved in the clathrin light chain B (CLB) neuron-specific EN exon inclusion [47], and 9G8 and SF2/ASF bind specifically to the FP element in the last exon of the bovine growth hormone (bGH) pre-mRNA, promoting its inclusion [62]. Like the ESS and ESE described here, other exons exhibit redundant and overlapping target sites for different SR proteins. Multiple SF2/ASF binding sites within the FP element are required for maximal enhancing activity *in vitro* [63]. We have preliminary biochemical evidence on the interaction of SR and hnRNP proteins with some of these target sites in the ESS, in the ESE, and the splice sites flanking the  $\alpha$  exon (data not shown).

In non-epithelial cells, the preferred route of splicing was skipping of the  $\alpha$  exon. This could be explained by the relative strengths of the competing 5' splice sites (e.g. Refs. [26,59,64]) and the lack of regulatory elements within the  $\alpha$  exon. Skipping of the weak  $\alpha$  exon is facilitated by the repressor component of the ESS, whereas its inclusion is mediated by the combined interaction of the activator component of the ESS, and the ESE [34]. Competing antagonizing epithelial cell factors might be participating as well, in a similar way as hnRNP A1 promotes skipping, and SF2/A2F promotes inclusion of the CLB neuron-specific EN exon [47]. This could be achieved by selection of alternative 5' splice sites [65] or by differential binding specificities of the factors involved [66]. We can envisage a competence, possibly by steric hindrance, between splicing factors for the repressor and activator portions of the ESS. Furthermore, in the absence of both the ESS and the ESE elements, partially spliced intermediaries were rescued, evidencing the possible first event of splicing. When the ESE was present alone, all possible transcripts were obtained. The sole presence of ESS resulted in unspliced precursors.

An interesting finding was the apparent need of the integrity of the minigene to maintain splicing efficiency. Except for point mutations, any deletion or substitution modified the amount of spliced products. The most dramatic effects were observed when the ends of the minigene were modified. Possibly, the factors required for splicing were not able to interact as well as with the intact transcripts, or the overexpressed modified transcripts titrated out the necessary factors to carry out the alternative splicing of the  $\alpha$  exon. Also, the amount of transcripts obtained from several constructs differed from the wild type. Probably, the promoter structure of such constructs differed from wild type, thus modifying the rate of splicing [67], or each construct may be recruiting slightly different splicing machinery components, thus stimulating RNA polymerase II transcription and processivity differently [68], in a reciprocal synergistic manner [69].

Finally, the splicing machinery of epithelial cells reversed the behavior observed for our constructs in neural cells where splicing factors could be in limiting amounts. This differential behavior between cell lines parallels ZO-1 $\alpha$ / $\alpha$  – expression during mouse blastocyst formation. Although ZO-1 is embryonically synthesized after the mouse genome activates at the 2-cell stage [70], TJ formation in mouse begins during compaction at the 8-cell stage and is complete by cavitation (blastocoel formation) at the 32-cell stage [71–73]. In the trophectoderm lineage, ZO-1 $\alpha$  – is expressed early in development and ZO-1 $\alpha$ + is first expressed before 32-cell stage [48]. In knock-out mice, for the essential and non-redundant SRp20 splicing factor, blastocyst formation is blocked at the 32-cell stage [74].

In conclusion, the alternative splicing of  $\alpha$  exon requires a multiple-step combinatorial control to maintain the delicate balance between both ZO-1 isoforms expressed at one time in epithelial cells. This process involves the weak splice sites flanking the  $\alpha$  exon, and two exonic antagonistic control elements, localized in the flanking constitutive exons, with no resemblance to previously reported splicing enhancers/silencers.

## Acknowledgements

We are grateful to C.W.J. Smith and B. Chabot for helpful comments, to Douglas L. Black for the DUP4-1 plasmid, and to Jorge Martínez-Alvarado for technical assistance. This work was supported by CONACYT-México: grants 26385-M and 30595-N, and PhD scholarship to R.M.-C.

## References

[1] C.W. Smith, E.B. Porro, J.G. Patton, B. Nadal-Ginard, Scanning from an independently specified branch point defines the 3' splice site of mammalian introns, *Nature* 342 (1989) 243–247.  
 [2] J. Valcárcel, R. Singh, M.R. Green, Mechanisms of regulated Pre-

mRNA splicing, in: A.I. Lamond (Ed.), *Pre-mRNA Processing*, R.G. Landes Co., New York, NY, 1995, pp. 97–112.  
 [3] L. Croft, S. Schandorff, F. Clark, K. Burrage, P. Arctander, J.S. Mattick, *Nat. Genet.* 24 (2000) 340.  
 [4] E.S. Lander, L.M. Linton, B. Birren, C. Nusbaum, M.C. Zody, J. Baldwin, K. Devon, K. Dewar, M. Doyle, W. FitzHugh, R. Funke, et al., Initial sequencing and analysis of the human genome, *Nature* 409 (2001) 860–921.  
 [5] D.L. Black, Finding splice sites within a wilderness of RNA, *RNA* 1 (1995) 763–771.  
 [6] B. Chabot, Directing alternative splicing: cast and scenarios, *Trends Genet.* 12 (1996) 472–478.  
 [7] A.J. Lopez, Alternative splicing of pre-mRNA: developmental consequences and mechanisms of regulation, *Annu. Rev. Genet.* 32 (1998) 279–305.  
 [8] G.S. Huh, R.O. Hynes, Regulation of alternative pre-mRNA splicing by a novel repeated hexanucleotide element, *Genes Dev.* 8 (1994) 1561–1574.  
 [9] H. Lou, R.F. Gagel, S.M. Berget, An intron enhancer recognized by splicing factors activates polyadenylation, *Genes Dev.* 10 (1996) 208–219.  
 [10] E.F. Modafferi, D.L. Black, A complex intronic splicing enhancer from the c-src pre-mRNA activates inclusion of a heterologous exon, *Mol. Cell. Biol.* 17 (1997) 6537–6545.  
 [11] C. Gooding, G.C. Roberts, C.W. Smith, Role of an inhibitory pyrimidine element and polypyrimidine tract binding protein in repression of a regulated alpha-tropomyosin exon, *RNA* 4 (1998) 85–100.  
 [12] J. Côté, S. Dupuis, Z. Jiang, J.Y. Wu, Caspase-2 pre-mRNA alternative splicing: Identification of an intronic element containing a decoy 3' acceptor site, *Proc. Natl. Acad. Sci. U. S. A.* 98 (2001) 938–943.  
 [13] C.C. van Oers, G.J. Adema, H. Zandberg, T.C. Moen, P.D. Baas, Two different sequence elements within exon 4 are necessary for calcitonin-specific splicing of the human calcitonin/calcitonin gene-related peptide I pre-mRNA, *Mol. Cell. Biol.* 14 (1994) 951–960.  
 [14] M.B. Humphrey, J. Bryan, T.A. Cooper, S.M. Berget, A 32-nucleotide exon-splicing enhancer regulates usage of competing 5' splice sites in a differential internal exon, *Mol. Cell. Biol.* 15 (1995) 3979–3988.  
 [15] J. Ramchatesingh, A.M. Zahler, K.M. Neugebauer, M.B. Roth, T.A. Cooper, A subset of SR proteins activates splicing of the cardiac troponin T alternative exon by direct interactions with an exonic enhancer, *Mol. Cell. Biol.* 15 (1995) 4898–4907.  
 [16] A. Staffa, A. Cochrane, Identification of positive and negative splicing regulatory elements within the terminal tat-rev exon of human immunodeficiency virus type 1, *Mol. Cell. Biol.* 15 (1995) 4597–4605.  
 [17] R.R. Gontarek, D. Derse, Interactions among SR proteins, an exonic splicing enhancer, and a lentivirus Rev protein regulate alternative splicing, *Mol. Cell. Biol.* 16 (1996) 2325–2331.  
 [18] A. Hanamura, J.F. Caceres, A. Mayeda, B.R. Franza Jr., A.R. Krainer, Regulated tissue-specific expression of antagonistic pre-mRNA splicing factors, *RNA* 4 (1998) 430–444.  
 [19] O. Nayler, C. Cap, S. Stamm, Human transformer-2-beta gene (SFRS10): complete nucleotide sequence, chromosomal localization, and generation of a tissue-specific isoform, *Genomics* 53 (1998) 191–202.  
 [20] E. Stickeler, F. Kittrell, D. Medina, S.M. Berget, Stage-specific changes in SR splicing factors and alternative splicing in mammary tumorigenesis, *Oncogene* 18 (1999) 3574–3582.  
 [21] J.Y. Seong, S. Park, K. Kim, Enhanced splicing of the first intron from the gonadotropin-releasing hormone (GnRH) primary transcript is a prerequisite for mature GnRH messenger RNA: presence of GnRH neuron-specific splicing factors, *Mol. Endocrinol.* 13 (1999) 1882–1895.  
 [22] V.C. Hou, R. Lersch, S.L. Gee, J.L. Ponthier, A.J. Lo, M. Wu, C.W. Turck, M. Koury, A.R. Krainer, A. Mayeda, J.G. Conboy, Decrease in

- hnRNP A/B expression during erythropoiesis mediates a pre-mRNA splicing switch, *EMBO J.* 21 (2002) 6195–6204.
- [23] M.D. Robida, R. Singh, *Drosophila* polypyrimidine-tract binding protein (PTB) functions specifically in the male germ line, *EMBO J.* 22 (2003) 2924–2933.
- [24] R.D. Phair, T. Misteli, High mobility of proteins in the mammalian cell nucleus, *Nature* 404 (2000) 604–609.
- [25] J.F. Cáceres, G.R. Sreaton, A.R. Krainer, A specific subset of SR proteins shuttles continuously between the nucleus and the cytoplasm, *Genes Dev.* 12 (1998) 55–66.
- [26] G.S. Huh, R.O. Hynes, Elements regulating an alternatively spliced exon of the rat fibronectin gene, *Mol. Cell. Biol.* 13 (1993) 5301–5314.
- [27] M. Caputi, G. Casari, S. Guenzi, R. Tagliabue, A. Sidoli, C.A. Melo, F.E. Baralle, A novel bipartite splicing enhancer modulates the differential processing of the human fibronectin EDA exon, *Nucleic Acids Res.* 22 (1994) 1018–1022.
- [28] K.W. Lynch, T. Maniatis, Assembly of specific SR protein complexes on distinct regulatory elements of the *Drosophila* doublesex splicing enhancer, *Genes Dev.* 10 (1996) 2089–2101.
- [29] M. Ashiya, P.J. Grabowski, A neuron-specific splicing switch mediated by an array of pre-mRNA repressor sites: evidence of a regulatory role for the polypyrimidine tract binding protein and a brain-specific PTB counterpart, *RNA* 3 (1997) 996–1015.
- [30] M. Blanchette, B. Chabot, A highly stable duplex structure sequesters the 5' splice site region of hnRNP A1 alternative exon 7B, *RNA* 3 (1997) 405–419.
- [31] J. Côté, M.J. Simard, B. Chabot, An element in the 5' common exon of the NCAM alternative splicing unit interacts with SR proteins and modulates 5' splice site selection, *Nucleic Acids Res.* 27 (1999) 2529–2537.
- [32] M.Y. Chou, N. Rooke, C.W. Turck, D.L. Black, hnRNP H is a component of a splicing enhancer complex that activates a c-src alternative exon in neuronal cells, *Mol. Cell. Biol.* 19 (1999) 69–77.
- [33] E.F. Modafferi, D.L. Black, Combinatorial control of a neuron-specific exon, *RNA* 5 (1999) 687–706.
- [34] C.W. Smith, J. Valcarcel, Alternative pre-mRNA splicing: the logic of combinatorial control, *Trends Biochem. Sci.* 25 (2000) 381–388.
- [35] L. González-Mariscal, S. Islas, R.G. Contreras, M.R. García-Villegas, A. Betanzos, J. Vega, A. Díaz-Quinónez, N. Martín-Orozco, V. Ortiz-Navarrete, M. Cerejido, J. Valdés, Molecular characterization of the tight junction protein ZO-1 in MDCK cells, *Exp. Cell Res.* 248 (1999) 97–109.
- [36] E. Willott, M.S. Balda, M. Heintzelman, B. Jameson, J.M. Anderson, Localization and differential expression of two isoforms of the tight junction protein ZO-1, *Am. J. Physiol.* 262 (1992) C1119–C1124.
- [37] M.S. Balda, J.M. Anderson, Two classes of tight junctions are revealed by ZO-1 isoforms, *Am. J. Physiol.* 264 (1993) C918–C924.
- [38] J.L. Underwood, C.G. Murphy, J. Chen, L. Franse-Carman, I. Wood, D.L. Epstein, J.A. Alvarado, Glucocorticoids regulate transendothelial fluid flow resistance and formation of intercellular junctions, *Am. J. Physiol.* 277 (1999) C330–C342.
- [39] J.M. Diamond, Tight and leaky junctions of epithelia: a perspective on kisses in the dark, *Fed. Proc.* 33 (1974) 2220–2224.
- [40] L. Reuss, Tight junction permeability to ions and water, in: M. Cerejido (Ed.), *Tight Junctions*, CRC Press, Boca Raton, 1992, pp. 49–66.
- [41] M. Cerejido, J. Valdés, L. Shoshani, R.G. Contreras, Role of tight junctions in establishing and maintaining cell polarity, *Annu. Rev. Physiol.* 60 (1998) 161–177.
- [42] E. Willott, M.S. Balda, A.S. Fanning, B. Jameson, C. Van Itallie, J.M. Anderson, The tight junction protein ZO-1 is homologous to the *Drosophila* discs-large tumor suppressor protein of septate junctions, *Proc. Natl. Acad. Sci. U. S. A.* 90 (1993) 7834–7838.
- [43] M. Itoh, A. Nagafuchi, S. Yonemura, T. Kitani-Yasuda, S. Tsukita, S. Tsukita, The 220-kD protein colocalizing with cadherins in non-epithelial cells is identical to ZO-1, a tight junction-associated protein in epithelial cells: cDNA cloning and immunoelectron microscopy, *J. Cell Biol.* 121 (1993) 491–502.
- [44] R.G. Contreras, A. Lazaro, J.J. Bolívar, C. Flores-Maldonado, S.H. Sánchez, L. González-Mariscal, M.R. García-Villegas, J. Valdés, M. Cerejido, A novel type of cell–cell cooperation between epithelial cells, *J. Membr. Biol.* 145 (1995) 305–310.
- [45] J. Sambrook, E.F. Fritsch, T. Maniatis, *Molecular cloning: a laboratory manual*, Cold Spring Harbor Laboratory Press, Cold Spring Harbor, NY, 1989.
- [46] P. Chomczynski, N. Sacchi, Single-step method of RNA isolation by acid guanidinium thiocyanate–phenol–chloroform extraction, *Anal. Biochem.* 162 (1987) 156–159.
- [47] J.F. Cáceres, S. Stamm, D.M. Helfman, A.R. Krainer, Regulation of alternative splicing in vivo by overexpression of antagonistic splicing factors, *Science* 265 (1994) 1706–1709.
- [48] B. Sheth, I. Fesenko, J.E. Collins, B. Moran, A.E. Wild, J.M. Anderson, T.P. Fleming, Tight junction assembly during mouse blastocyst formation is regulated by late expression of ZO-1 alpha+ isoform, *Development* 124 (1997) 2027–2037.
- [49] Y.A. Zhuang, A.M. Goldstein, A.M. Weiner, UACUAAAC is the preferred branch site for mammalian mRNA splicing, *Proc. Natl. Acad. Sci. U. S. A.* 86 (1989) 2752–2756.
- [50] C.B. Burge, T. Tuschl, P.A. Sharp, Splicing of precursors to mRNAs by the spliceosomes, in: R.F. Gesteland, T.R. Cech, J.F. Atkins (Eds.), *The RNA World*, Cold Spring Harbor Laboratory Press, Cold Spring Harbor, NY, 1999, pp. 525–560.
- [51] A. Staffa, A. Cochrane, The tat/rev intron of human immunodeficiency virus type 1 is inefficiently spliced because of suboptimal signals in the 3' splice site, *J. Virol.* 68 (1994) 3071–3079.
- [52] D.A. Sterner, S.M. Berget, In vivo recognition of a vertebrate mini-exon as an exon–intron–exon unit, *Mol. Cell. Biol.* 13 (1993) 2677–2687.
- [53] F. Del Gatto, A. Plet, M.C. Gesnel, C. Fort, R. Breathnach, Multiple interdependent sequence elements control splicing of a fibroblast growth factor receptor 2 alternative exon, *Mol. Cell. Biol.* 17 (1997) 5106–5116.
- [54] C.F. Kennedy, S.M. Berget, Pyrimidine tracts between the 5' splice site and branch point facilitate splicing and recognition of a small *Drosophila* intron, *Mol. Cell. Biol.* 17 (1997) 2774–2780.
- [55] J. Southby, C. Gooding, C.W. Smith, Polypyrimidine tract binding protein functions as a repressor to regulate alternative splicing of alpha-actinin mutually exclusive exons, *Mol. Cell. Biol.* 19 (1999) 2699–2711.
- [56] I. Perez, C.H. Lin, J.G. McAfee, J.G. Patton, Mutation of PTB binding sites causes misregulation of alternative 3' splice site selection in vivo, *RNA* 3 (1997) 764–778.
- [57] J.A. Berglund, M.L. Fleming, M. Rosbash, The KH domain of the branchpoint sequence binding protein determines specificity for the pre-mRNA branchpoint sequence, *RNA* 4 (1998) 998–1006.
- [58] S. Kammler, C. Leurs, M. Freund, J. Krummheuer, K. Seidel, T.O. Tange, M.K. Lund, J. Kjems, A. Scheid, H. Schaal, The sequence complementarity between HIV-1 5' splice site SD4 and U1 snRNA determines the steady-state level of an unstable env pre-mRNA, *RNA* 7 (2001) 421–434.
- [59] L.P. Eperon, J.P. Estibeiro, I.C. Eperon, The role of nucleotide sequences in splice site selection in eukaryotic pre-messenger RNA, *Nature* 324 (1986) 280–282.
- [60] A. Staffa, N.H. Acheson, A. Cochrane, Novel exonic elements that modulate splicing of the human fibronectin EDA exon, *J. Biol. Chem.* 272 (1997) 33394–33401.
- [61] C.E. Chalfant, J.E. Watson, L.D. Bisnauth, J.B. Kang, N. Patel, L.M. Obeid, D.C. Eichler, D.R. Cooper, Insulin regulates protein kinase CbetaII expression through enhanced exon inclusion in L6 skeletal muscle cells. A novel mechanism of insulin- and insulin-like growth factor-i-induced 5' splice site selection, *J. Biol. Chem.* 273 (1998) 910–916.
- [62] X. Li, M.E. Shambaugh, F.M. Rottman, J.A. Bokar, SR proteins Asf/

- SF2 and 9G8 interact to activate enhancer-dependent intron D splicing of bovine growth hormone pre-mRNA in vitro, *RNA* 6 (2000) 1847–1858.
- [63] W.P. Dirksen, X. Li, A. Mayeda, A.R. Krainer, F.M. Rottman, Mapping the SF2/ASF binding sites in the bovine growth hormone exonic splicing enhancer, *J. Biol. Chem.* 275 (2000) 29170–29177.
- [64] Y. Zhuang, H. Leung, A.M. Weiner, The natural 5' splice site of simian virus 40 large T antigen can be improved by increasing the base complementarity to U1 RNA, *Mol. Cell. Biol.* 7 (1987) 3018–3020.
- [65] I.C. Eperon, O.V. Makarova, A. Mayeda, S.H. Munroe, J.F. Cáceres, D.G. Hayward, A.R. Krainer, Selection of alternative 5' splice sites: role of U1 snRNP and models for the antagonistic effects of SF2/ASF and hnRNP A1, *Mol. Cell. Biol.* 20 (2000) 8303–8318.
- [66] R. Tacke, J.L. Manley, The human splicing factors ASF/SF2 and SC35 possess distinct, functionally significant RNA binding specificities, *EMBO J.* 14 (1995) 3540–3551.
- [67] P. Cramer, C.G. Pesce, F.E. Baralle, A.R. Kornblihtt, Functional association between promoter structure and transcript alternative splicing, *Proc. Natl. Acad. Sci. U. S. A.* 94 (1997) 11456–11460.
- [68] H. Le Hir, A. Nott, M.J. Moore, How introns influence and enhance eukaryotic gene expression, *Trends Biochem. Sci.* 28 (2003) 215–220.
- [69] Y.W. Fong, Q. Zhou, Stimulatory effect of splicing-factors on transcriptional elongation, *Nature* 414 (2001) 929–933.
- [70] T.P. Fleming, M.J. Hay, Tissue-specific control of expression of the tight junction polypeptide ZO-1 in the mouse early embryo, *Development* 113 (1991) 295–304.
- [71] T. Ducibella, D.F. Albertini, E. Anderson, J.D. Biggers, The preimplantation mammalian embryo: characterization of intercellular junctions and their appearance during development, *Dev. Biol.* 45 (1975) 231–250.
- [72] T. Magnuson, A. Demsey, C.W. Stackpole, Characterization of intercellular junctions in the preimplantation mouse embryo by freeze-fracture and thin-section electron microscopy, *Dev. Biol.* 61 (1977) 252–261.
- [73] T.P. Fleming, J. McConnell, M.H. Johnson, B.R. Stevenson, Development of tight junctions de novo in the mouse early embryo: control of assembly of the tight junction-specific protein ZO-1, *J. Cell Biol.* 108 (1989) 1407–1418.
- [74] H. Jumaa, G. Wei, P.J. Nielsen, Blastocyst formation is blocked in mouse embryos lacking the splicing factor SRp20, *Curr. Biol.* 9 (1999) 899–902.
- [75] K.W. Lynch, T. Maniatis, Synergistic interactions between two distinct elements of a regulated splicing enhancer, *Genes Dev.* 9 (1995) 284–293.
- [76] P. Sirand-Pugnet, P. Durosay, E. Brody, J. Marie, An intronic (A/U)GGG repeat enhances the splicing of an alternative intron of the chicken beta-tropomyosin pre-mRNA, *Nucleic Acids Res.* 23 (1995) 3501–3507.
- [77] D.M. Standiford, M.B. Davis, W. Sun, C.P. Emerson Jr., Splice-junction elements and intronic sequences regulate alternative splicing of the *Drosophila* myosin heavy chain gene transcript, *Genetics* 147 (1997) 725–741.
- [78] E. Labourier, E. Allemand, S. Brand, M. Fostier, J. Tazi, H.M. Bourbon, Recognition of exonic splicing enhancer sequences by the *Drosophila* splicing repressor RSF1, *Nucleic Acids Res.* 27 (1999) 2377–2386.